# Spread Footings in Sand: Load Settlement Curve Approach

Jean-Louis Briaud[1]

**Abstract:** A study of the assumptions involved in the ultimate bearing capacity equation indicates the shortcomings of that equation and load test data confirm these shortcomings. A new approach using a normalized load settlement curve is proposed to alleviate these shortcomings and to obtain the complete load settlement curve for a footing in sand. The normalization consists of plotting the mean footing pressure divided by a measure of the soil strength within the depth of influence of the footing versus the settlement divided by the footing width. It is shown that the normalized load settlement curve for a footing is independent of footing size and embedment. It is proposed to obtain the normalized curve point-by-point from a soil test. Because the deformation of the soil observed under full-scale footings during loading indicates a barreling effect similar to the soil deformation around a pressuremeter probe, the preboring pressuremeter curve is used to obtain the footing curve. The new method consists of transforming the preboring pressuremeter curve point-by-point into the footing load settlement curve. Load tests and numerical simulations are used to propose a method for a rectangular footing near a slope subjected to an eccentric and inclined load. The new method gives the complete load settlement curve for the footing and alleviates the problems identified with the bearing capacity equation.

**DOI:** 10.1061/(ASCE)1090-0241(2007)133:8(905)

**CE Database subject headings:** Sand; Spread foundations; Bearing capacity; Foundation settlement; Load tests; Simulation; Curvature.

## Introduction

In many instances, spread footings are more economical than piles. For example, in the case of bridges where the cost of the foundation is often as high as 50% of the total cost, it is not unusual to be able to save 50% of the foundation cost if spread footings are used instead of piles. The potential savings that would be derived by providing added information to the engineer on the behavior of spread footings in sand was the impetus for this 12-year-long research program. It included performing very large-scale spread footing tests, extensive numerical simulations, and a study of existing knowledge including the ultimate bearing capacity equation, the elasticity equation for settlement of a footing, and existing footing load test data.

The goal of the research was to develop a method that would give a complete load settlement curve for the footing, thereby providing continuity between the common approach of considering separately ultimate bearing capacity and settlement. The approach consisted of transforming a pressuremeter curve representative of the soil below the footing into a load settlement curve for that footing. The reason for selecting the pressuremeter curve was that observations made during full-scale footing load tests showed that the soil below the footing deformed by lateral expansion, as in the case of a pressuremeter test. The transformation between the pressuremeter curve and the footing load settlement curve proposed in this article is based on 24 footing load tests with parallel pressuremeter tests, on 15 three-dimensional nonlinear numerical simulations, and on the study of the elasticity settlement equation and the ultimate bearing capacity equation.

[1]Spencer J. Buchanan Chair, Dept. of Civil Engineering, Texas A&M Univ, College Station, TX 77834-3136. E-mail: briaud@tamu.edu

Note. Discussion open until January 1, 2008. Separate discussions must be submitted for individual papers. To extend the closing date by one month, a written request must be filed with the ASCE Managing Editor. The manuscript for this paper was submitted for review and possible publication on December 13, 2004; approved on August 25, 2006. This paper is part of the ***Journal of Geotechnical and Geoenvironmental Engineering***, Vol. 133, No. 8, August 1, 2007. ©ASCE, ISSN 1090-0241/2007/8-905–920/$25.00.

## Ultimate Bearing Capacity Equation

The ultimate bearing capacity equation for a strip footing in a uniform sand (no cohesion) states that (Terzaghi et al. 1996)

$$q_u = 0.5\gamma B N_\gamma + \gamma D N_q \quad (1)$$

where $q_u$=ultimate bearing capacity ($kN \cdot m^2$); $\gamma$=effective unit weight ($kN \cdot m^3$); $B$=width of the footing (m); $D$=depth of embedment (m); and $N_\gamma$ and $N_q$=bearing capacity factors, which are a function of the effective stress friction angle $\varphi$. Eq. (1) indicates that $q_u$ increases linearly with $B$ or $D$.

There seems to be an unresolved debate on some of the shortcomings of Eq. (1) including the fact that spread footing load tests do not always follow the trend of linear increase with $B$ or $D$ (Briaud and Gibbens 1999). Many researchers have studied this discrepancy and proposed various explanations. Explanations due to nonlinearity of the failure envelope were proposed by DeBeer (1965, 1970), Ovesen (1975), Graham and Hovan (1986), Hettler and Gudehus (1988), Kutter et al. (1988), Bolton and Lau (1989), and Shiraishi (1990). Explanations due to progressive failure were proposed by Muhs (1965) and Yamaguchi et al. (1976) due to dilatancy by Bolton (1986), due to the ratio between the footing size and the grain size by Steenfelt (1977), and due to other factors by Corte (1980), Habib (1985), Kimura et al. (1985), Garnier (1997), and Perkins and Madson (2000). In this article, a different and very simple reason is given to explain the difference between experimental observations and the theory.

Three of the hypotheses on which Eq. (1) is based are (Terzaghi 1943): $\varphi$ is constant with depth, $\gamma$ is constant with depth, and

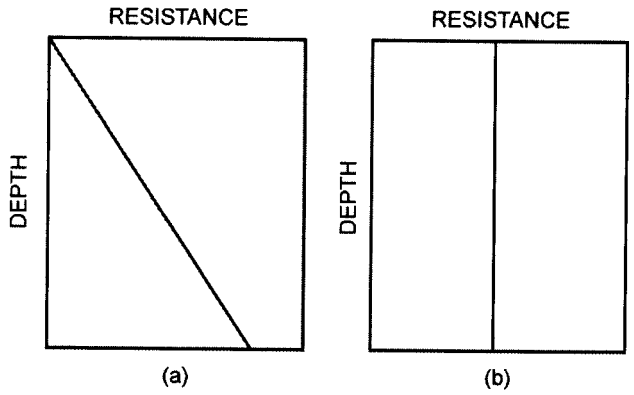


**Fig. 1.** Two types of soil strength profiles: (a) linear increase; (b) constant

the soil is dry. Therefore the effective stress $\sigma'$ and the shear strength $\tau_f$ increase linearly with depth [Fig. 1(a)] since

$$\tau_f = \sigma' \tan \phi \tag{2}$$

Eq. (1) should predict the ultimate bearing capacity with good accuracy when the soil strength increases linearly with depth. An standard penetration test (SPT) profile, a cone penetration test (CPT) profile, or a pressure meter test (PMT) limit pressure profile can be used to determine if such an assumption is verified at a given site. However, close to the ground surface where spread footings are often founded, soils are unsaturated or saturated by capillary action and strength profiles are constant with depth. This is due to the fact that the total stress increases with depth while the suction decreases with depth at a rate such that the stress between the grains is approximately constant. In the case of a constant strength profile also, one can expect that the ultimate bearing capacity will not vary with the footing width or the depth of embedment since the strength is constant within the zone of influence of the footing. This discussion shows that the soil strength profile is likely to have an impact on the scale effect and the embedment effect for a footing on sand. It also indicates that Eq. (1) is limited to cases where the soil strength increases linearly with depth since this is consistent with the assumptions on which it is based.

## Elasticity Equation for Settlement

The theory of elasticity is often used to estimate the settlement of spread footings on sand. The equation (Mayne and Poulos 1999)

$$s = (qB/E)(1 - \nu^2) I_G I_F I_E \tag{3}$$

where the settlement $s$=function of the mean footing pressure $q$; diameter $B$=circular footing; and the soil's Young modulus $E$ and Poisson's ratio $\nu$, and the factors $I_E$ (Fig. 2), $I_F$, and $I_G$ (Fig. 3) =influence of the footing embedment, the footing flexibility, and the increase in modulus versus depth, respectively. For a rigid circular foundation at the surface of a soil with constant modulus $E$, Eq. (3) becomes

$$s = (qB/E)(1 - \nu^2)\pi/4 \tag{4}$$

According to this equation and for a given footing shape, the $q$ versus $s/B$ curve will be independent of the footing size and will depend only on the soil properties $E$ and $\nu$. On the other hand, the $I_E$ factor (Fig. 2) shows that increasing the embedment decreases the settlement. The maximum decrease varies from 10 to 15% for reasonable values of the Poisson's Ratio (0.3 to 0.5) and for common embedment values ($D/B$ from 0 to 2).

Consider now a rigid footing resting on a soil for which the modulus varies from $E_0$ at the ground surface to $2E_0$ at a depth of $2B$. In this case, $\beta$ in Fig. 2 is equal to 2 and $I_G$ to 0.59. If we now consider a footing which has a width $2B$ resting on the same soil, $\beta$ is 1, and $I_G$ is 0.5. If the scale effect is defined as the ratio of the two $s/B$ values, this ratio is simply the ratio of the two $I_G$ values [Eq. (3)] or 0.85 for a 15% difference.

This discussion on the elastic settlement shows that the modulus profile with depth has a direct influence on the scale and embedment effect. Furthermore, it shows that, for average conditions, the influence is small (<15%). In order to further quantify the influence of the strength and modulus profiles on the scale effect and the embedment effects, spread footing load test data were accumulated.

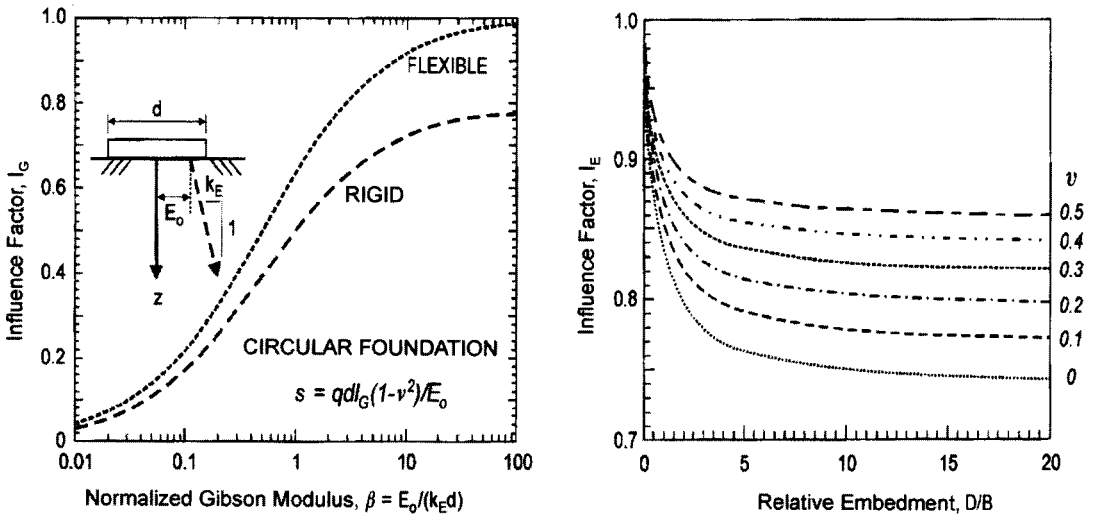


**Fig. 2.** Influence factors $I_G$ and $I_E$ (adapted from Mayne and Poulos 1999)

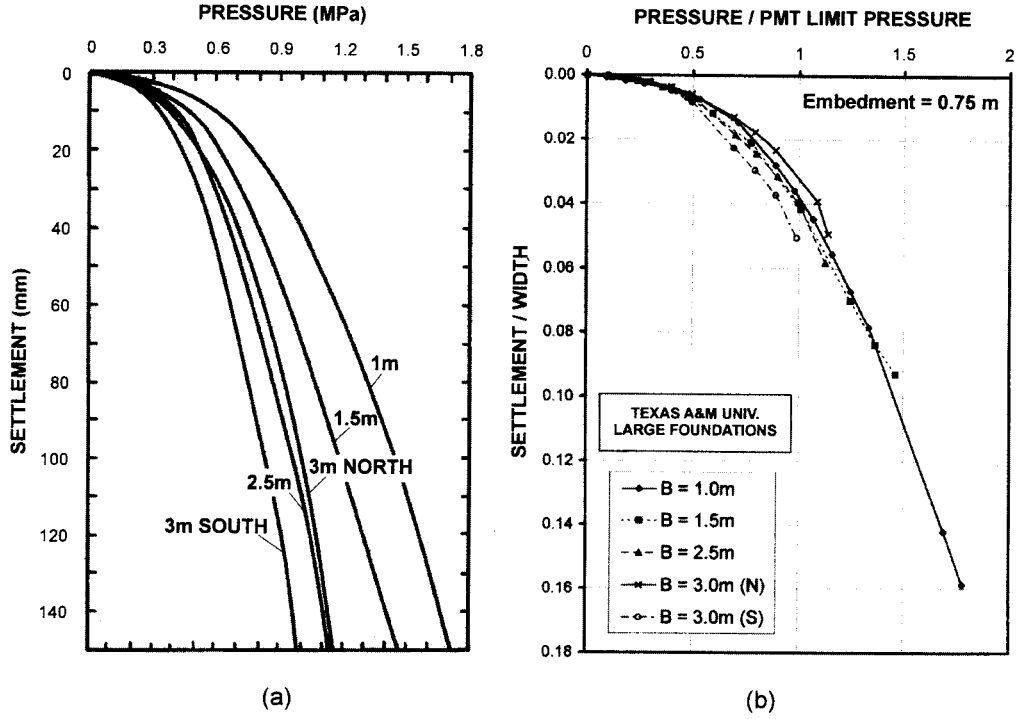


**Fig. 3.** Texas A&M University footing test results (adapted from Briaud and Gibbens 1999)

## Uniqueness of the Normalized Load Settlement Curve

Considering the theoretical observations made on the ultimate bearing capacity equation and the elasticity equation, it was decided to plot the load-settlement curve as mean footing pressure $p$ divided by a measure of the soil strength ($N$, $q_c$, $p_L$) within the depth of influence of the footing versus the settlement s divided by the footing width $B$. Note that $s/B$ is one half of the mean normal vertical strain within the depth of influence of the footing since $s$=displacement and $2B$ the depth within which this displacement is occurring. Note also that the normalization of $p$ by $N$ does not make the ratio nondimensional but does normalize the pressure by a quantity indicative of the soil strength. The choice of strength parameter used in the normalization process was dictated by what parameter was available for that case history. The hope was that with such a normalization, the curve would become independent of the scale effect and embedment effect. To investigate the effect of such a normalization, the results of footing load tests were sought where footing size and footing embedment had been varied and where the normalized curve could be constructed. Five independent studies from three different countries were found and are described next.

### *Texas A&M University Large-Scale Footing Tests (Briaud and Gibbens, 1999)*

Briaud and Gibbens (1999) used five concrete footings sized 1 $\times$1, 1.5$\times$1.5, 2.5$\times$2.5, 3$\times$3, and 3$\times$3 m, all 1.5-m-thick, and embedded 0.75 m in a silty sand with a relatively constant profile of SPT blow count equal to 20 bpf. The water table was 4.9-m deep. The pressure versus settlement curves obtained from the load tests are shown in Fig. 3(a). The pressure under the footing was normalized by the average limit pressure of preboring pressuremeter tests performed within the depth of influence of the footing next to the footing. The settlement was normalized by the footing width. Fig. 3(b) shows that the normalization brings the five normalized curves into a narrow band. Therefore, in this case, the normalized curves are independent of footing width and can be represented by a unique curve.

### *Spread Footing Tests in Kuwait*

Ismael (1985) conducted eight tests on square footings with different widths (0.25–1 m) and with different embedments (0.5–2 m). The soil was a slightly silty sand with a relatively constant SPT blow count profile averaging 20 bpf (Ismael, personal e-mail communication). The water table was 2.8 m deep. Fig. 4 shows the normalized load settlement curves for the effect of footing size [Fig. 4(a)] and of footing embedment [Fig. 4(b)]; in both instances the four curves collapse into a narrow band. In this case, the normalized curves are independent of footing width and footing embedment and become a unique curve. Indeed the curve for the width effect is the same as the curve for the embedment effect.

### *FHwA Spread Footing Tests*

FHwA (Lutenegger) conducted three tests on square footings (width 0.91 m, embedment $D/B$ from 0 to 1). The soil was a clean sand compacted in layers in a large test pit 7.5$\times$6.5 $\times$3.5 m. The water table in the test pit was 2.1-m deep and the strength profile increased linearly with depth as measured by the pressuremeter limit pressure (from 0 at the surface to 550 kPa at 2-m depth). All the footing tests were performed at an embedment depth equal to 1.2 m. Fig. 5(a) shows the results of the load tests as pressure versus settlement over width curves. Fig. 5(b) shows that, after normalization of the footing pressure by the average

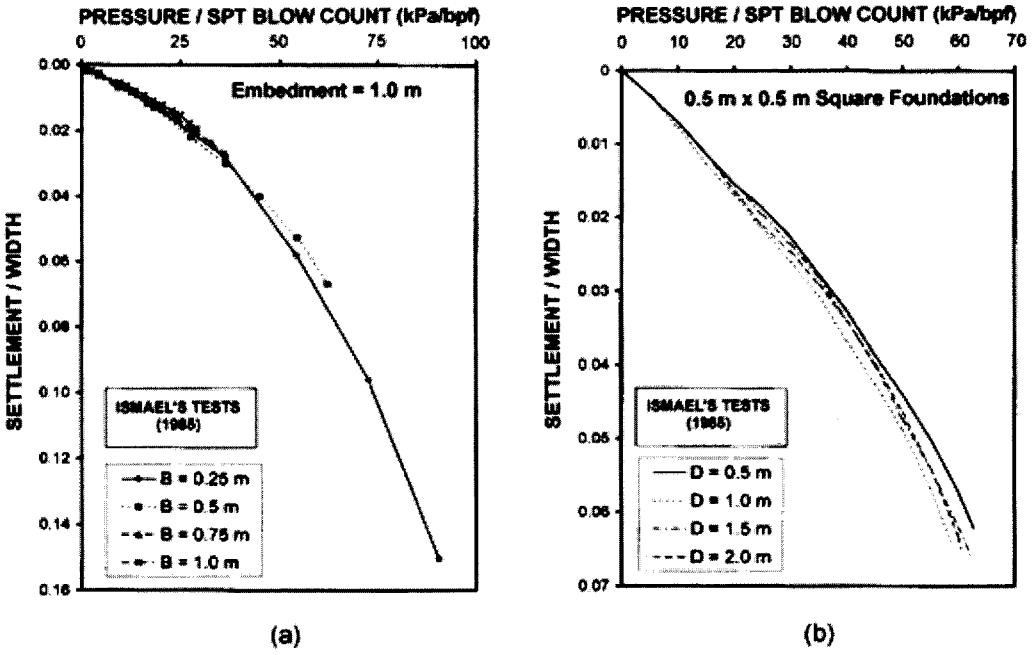


**Fig. 4.** Ismael (1985) footing tests results: (a) width influence; (b) embedment influence

limit pressure within the depth of influence of the footing ($p/p_l$), the three curves collapse into a narrow band. In this case, the normalized curves are independent of footing size and become a unique curve.

### *University of Colorado Centrifuge Footing Tests*

Pu and Ko (1988) conducted 5 footing tests in the University of Colorado centrifuge. The square footings were 25.4 mm in size and were tested at 50 g for a prototype dimension equal to 1.27 m. The footings were embedded at $D/B$ ratios equal to 0, 0.5, 1, 3, and 5. The soil was a clean sand with a strength profile starting at zero at the surface and increasing linearly with depth as measured by the CPT point resistance (Ko 1999, personal communication). Since the strength profile was increasing with depth like the vertical total stress in this dry sand, the normalization was done by dividing the average footing pressure by $1+(D/B)$, which is proportional to the stress at a depth equal to $1B$ below the foundation. Indeed the footing is buried at a depth $D$ and the

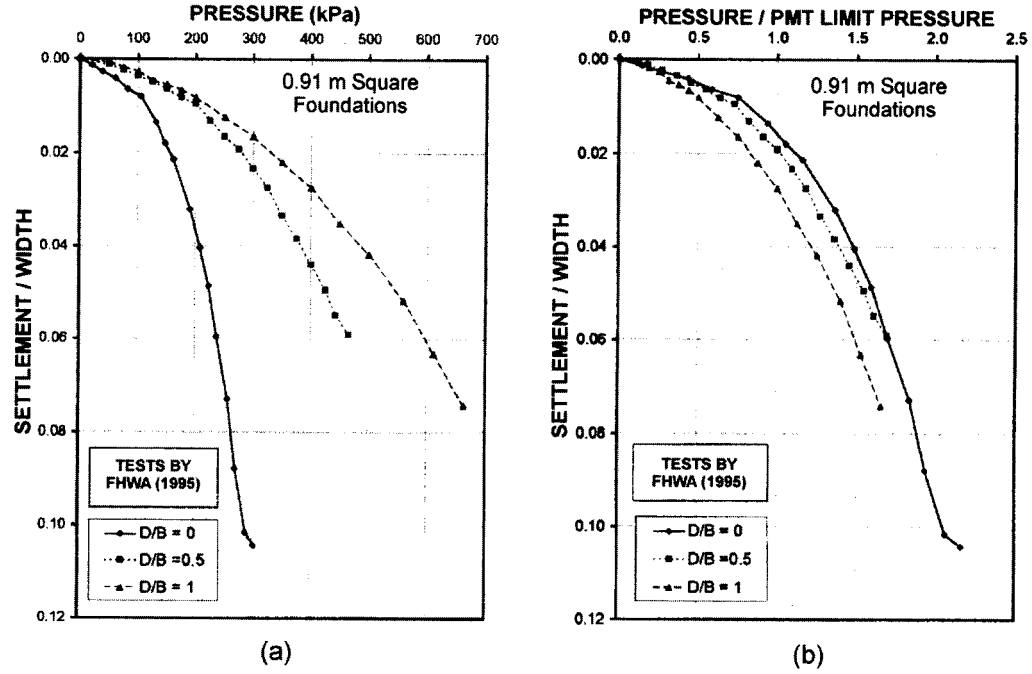


**Fig. 5.** FHwA footing tests results (via personal communication, Lutenegger, 1995): (a) nonnormalized curves; (b) normalized curves

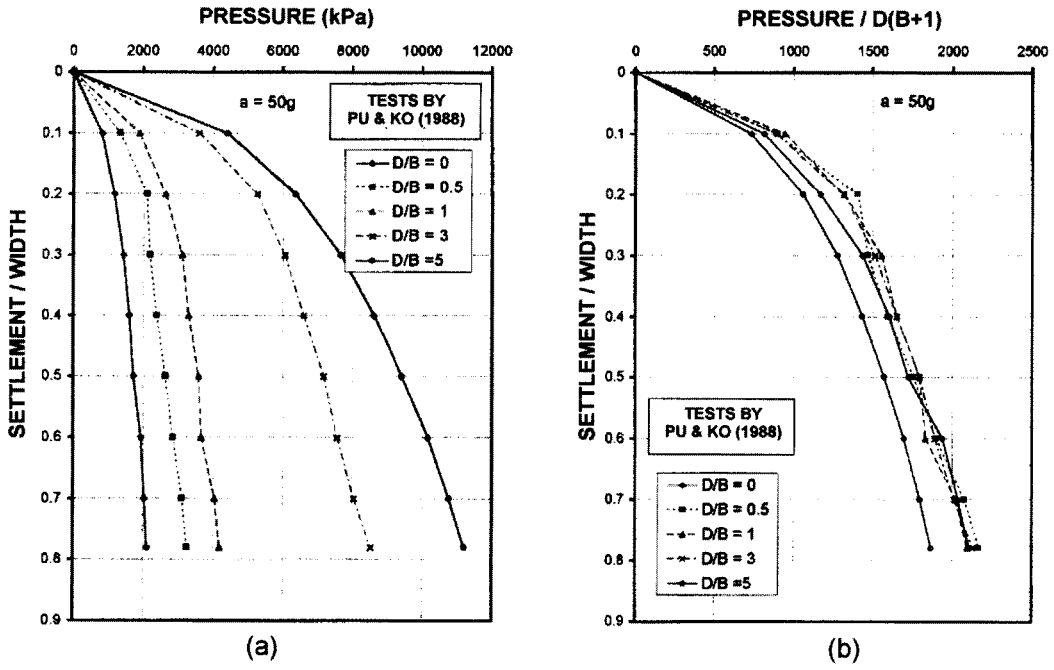


**Fig. 6.** University of Colorado footing tests results adapted from (Pu and Ko 1988): (a) nonnormalized curves; (b) normalized curves

zone of influence below a square footing is $2B$, so the quantity $(D+B)\gamma$=effective stress representative of the strength of this dry sand below the footing. Since $\gamma$=same for all tests and after dividing by $B$, which is the same for all tests, the quantity $(D+B)\gamma$ becomes $1+(D/B)$, which is proportional to the soil strength within the depth of influence. Fig. 6 shows the five load-settlement curves before and after normalization; the normalized curves collapse into a narrow band. In this case again, the normalized curves are independent of footing size and become a unique curve.

### *Spread Footing Tests in Brazil*

The soil in this case history is a clay not a sand, which is the topic of the article. It is shown here nevertheless because this clay case history shows the same behavior as the case histories on sand and indicates that a similar approach may also be valid for clays. Consoli et al. (1998) conducted five circular plate tests (diameter 0.3–0.6 m and three square footing tests (width 0.4–1 m). The soil was a silty and sandy clay with a cone point resistance averaging 500 kPa. All the tests were performed at an embedment depth equal to 1.2 m. Fig. 7 shows the eight pressure versus settlement curves and the eight normalized curves that collapse into a narrow band. The normalization is based on the unconfined compression strength. In this case, the normalized curves are independent of footing size and become a unique curve.

## New Load Settlement Curve Method

The previous experimental data and theoretical considerations give strong indications that the normalized load settlement curve is independent of scale and embedment. Therefore it was postulated that the curve could be obtained from a soil test alone for a reference footing case and that other factors such as shape, load eccentricity, load inclination, and proximity of a slope could be incorporated by using correction factors. This is similar to the bearing capacity equation, which exists for a reference case (strip footing), and is extended to the general case through multiplication by a series of influence factors. The choice of a soil test as a reference for the new method was based on the following observation. The inclinometer casing measurements made during the large scale footing tests at Texas A&M University showed that the deformation of the soil mass under the footing during loading was a barreling effect very much similar to the soil deformation around a preboring pressuremeter test during expansion (Briaud and Gibbens 1999). Therefore, an attempt was made to transform the normalized preboring PMT curve into the normalized load settlement curve for the footing (Fig. 8). The pressuremeter curve (Briaud 1992) gives the borehole pressure $p_p$ (boundary radial stress) versus the relative increase in cavity radius $\Delta R/R_0$ (boundary hoop strain). The footing curve is the average footing pressure $p_f$ versus the relative settlement $s/B$. The transformation was made on the basis of two equations, one aimed at matching strain levels between the two tests, the other aimed at transforming the pressures for that strain level

$$s/B = 0.24\Delta R/R_o \tag{5}$$

$$p_f = \Gamma p_p \tag{6}$$

where $s$=footing settlementl; $B$=footing width; $\Delta R$=increase in cavity radius in the PMT; $R_o$=initial radius of the PMT cavity; $p_f$=mean pressure under the footing when the settlement is $s$; $p_p$=pressure in the PMT when the increase in cavity radius is $\Delta R$; and $\Gamma$=Gamma function linking $p_p$ to $p_f$. Eq. (5) matches the strains at the ultimate values, which are $s/B$ equal to 0.1 for the footing (a typical reference) and $\Delta R/R_o$ equal to 0.414 for the PMT (corresponding to the definition of the limit pressure). Indeed the limit pressure for the pressuremeter is reached when the cavity volume has doubled; this corresponds to an increase in

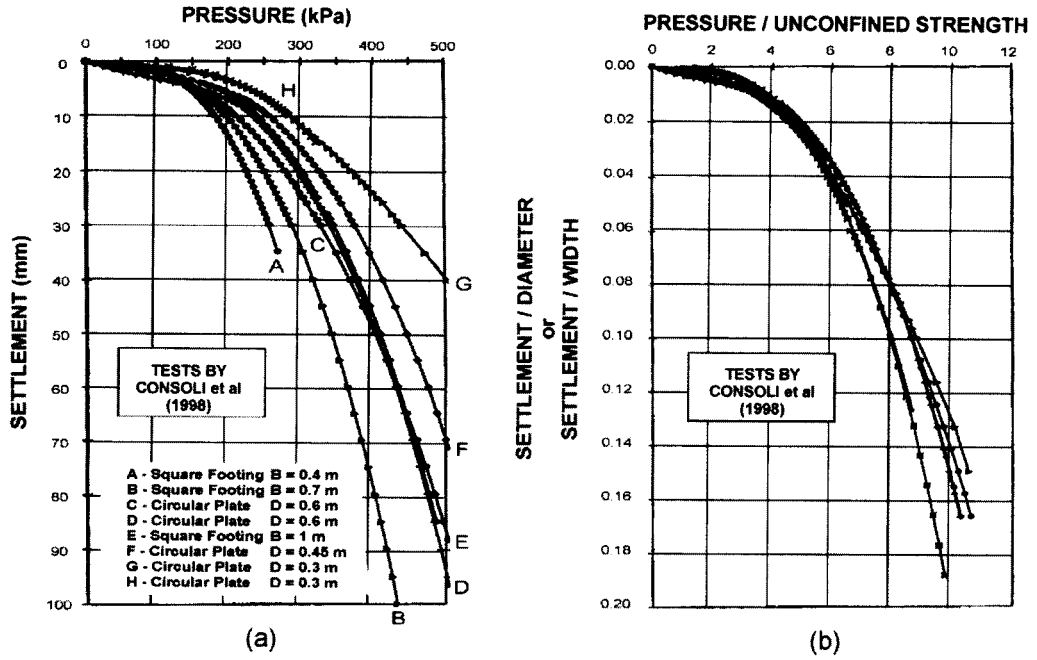


**Fig. 7.** Consoli et al. (1998) footing tests results: (a) nonnormalized curves; (b) normalized curves

cavity radius from $R_0$ to 1.414 $R_0$ or $\Delta R/R_o=0.414$. Then the ratio 0.1/0.414 is 0.24 in Eq. (5). The second equation is the pressure transformation equation which requires a function $\Gamma$. This function $\Gamma$ (Fig. 9) was originally found experimentally using the large scale Texas A&M University spread footing tests and parallel pressuremeter tests, and verified numerically using ABAQUS FEM simulations (Briaud and Jeanjean 1994). Later, the $\Gamma$ function was evaluated against other footing tests (Fig. 9) for which the load settlement curve and pressuremeter tests were available. The data presented in Fig. 9 comes from the following sources: Larsson 1997; Lutenegger 1995 (labeled FHWA in Fig. 9); Gibbens 1999 (labeled TAMU in Fig. 9); Despreles 1990; Khebib et al. 1997 (labeled LCPC in Fig. 9); Tand et al. 1994. The scatter gives the engineer an idea of the precision to expect

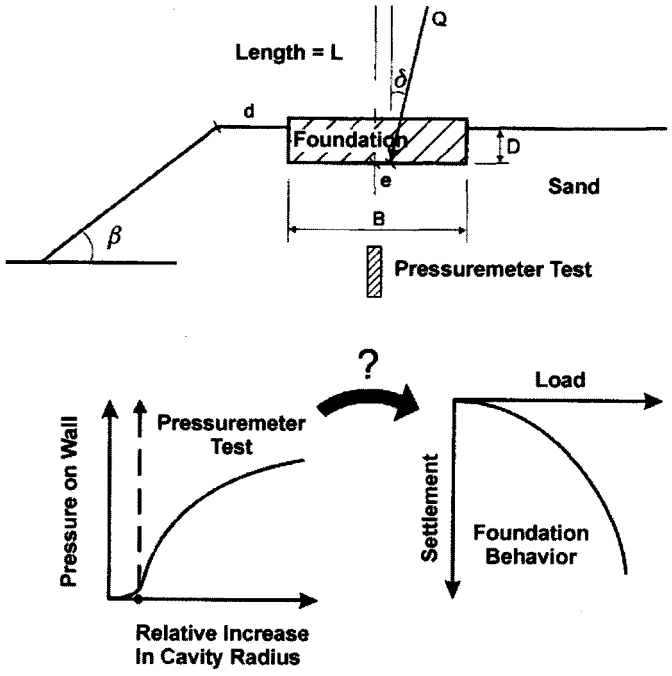


**Fig. 8.** Transforming the PMT curve into the spread footing load settlement curve

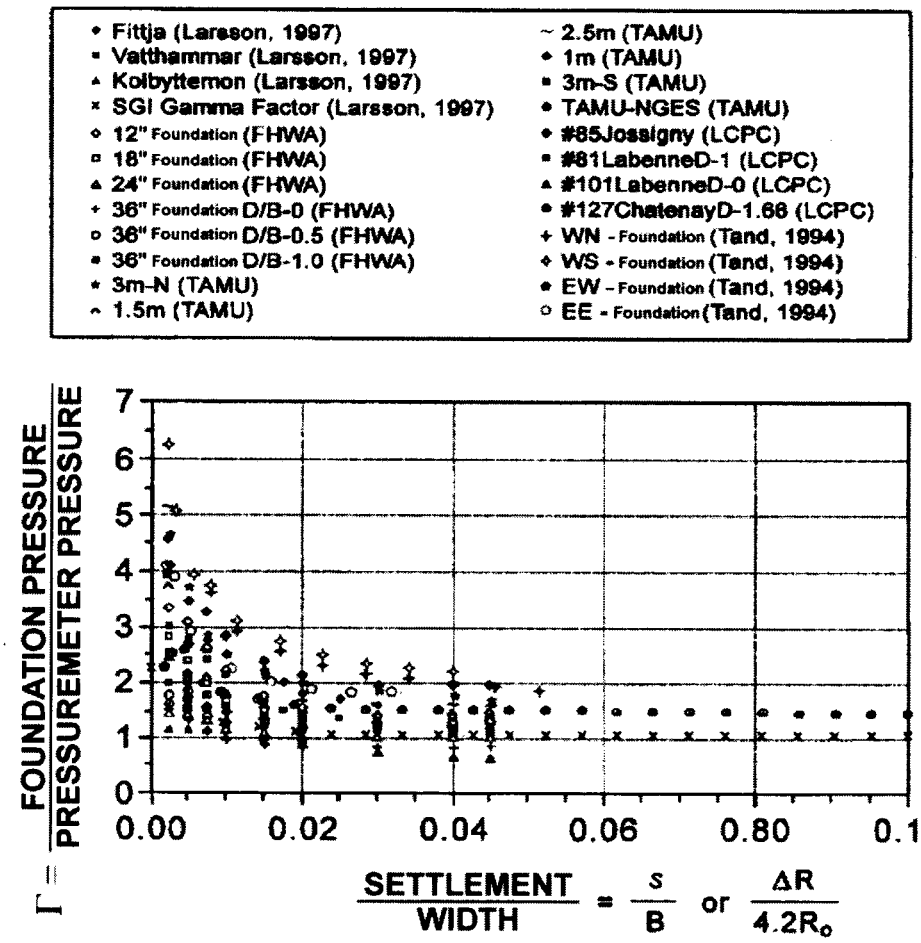


**Fig. 9.** Experimental determination of the Γ function

from the new method. Two Γ functions were identified (Fig. 10). The mean Γ function was obtained by taking the average of the Γ values on Fig. 9 for a given value of $s/B$ while the design Γ function was obtained by taking the mean minus one standard deviation of the Γ values in Fig. 9 for a given value of $s/B$.

## Influence Factors

The Γ function presented in the previous section refers to the case of a square footing loaded vertically at its center on a flat ground surface; this is called the reference case. In order to provide a solution for the more general case of a rectangular footing located near a slope and subjected to an eccentric and inclined load, several influence factors were developed to modify the Γ function. The factors were developed on the basis of three-dimensional nonlinear finite-element analyses (Hossain 1996) by varying one of the factors while keeping all others equal to the ones in the reference case. The program used was ABAQUS (1991), and the soil model was the Duncan–Chang hyperbolic model (Duncan and Chang 1970; Seed and Duncan 1983). The size of the mesh was $30B$ in all directions where $B$=footing width. The footing was also simulated with a thickness equal to 1 m and a size of $3\times3$ m. The bottom of the footing had a nonslip interface with the soil below and the side and bottom boundaries of the mesh were on rollers. The calibration of the model was achieved by matching the predicted load settlement curves with the load settlement curves measured for the large spread footing tests at Texas A&M University. The soil model parameters derived from this matching process (Table 1) were retained for all other simulations. The definition of all the Duncan–Chang model parameters in Table 1 can be found in Hossain (1996). The results obtained are associated and limited to the conditions simulated. Wherever possible, each influence factor is compared to measured data

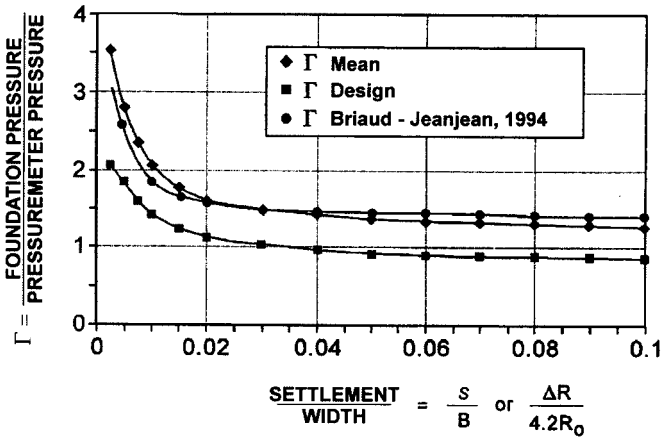


**Fig. 10.** Recommended Γ function

**Table 1.** Back-Calculated Values of the Soil Parameters for the Duncan–Chang Hyperbolic Model

| Modulus parameters | | Poisson's ratio parameters | | Other soil parameters | |
|---|---|---|---|---|---|
| $K$ | 3,500 | $G$ | 0.3 | $\gamma$ | 16 kN·m$^3$ |
| $\eta$ | 0.5 | $F$ | 0.0 | $K_0$ | 0.65 |
| $c$ | 0.0 | $A_g$ | 0.001 | | |
| $\phi$ | 31° | $A_f$ | 0.0 | | |
| $R_f$ | 0.92 | $B_g$ | 2.0 | | |
| $K_{ur}$ | 3500 | $B_f$ | 0.0 | | |

Note: Parameter definitions can be found in Hussain (1996).

found in the literature as well as existing recommendations for influence factors applying to the ultimate bearing capacity.

### Shape of the Foundation

Simulations were performed for $L/B$ ratios (length to width ratios) equal to 1, 2, 3, and 5. These simulations lead to predicted load settlement curves for the reference footing ($3\times3$ m) and for the rectangular footings being simulated (e.g., $3\times6$ m) (Fig. 11). If the $\Gamma$ function for a square footing is $\Gamma_{L/B=1}$ and if the $\Gamma$ function for a rectangular footing is $\Gamma_{L/B}$, then the ratio $\Gamma_{L/B}/\Gamma_{L/B=1}$=influence factor $f_{L/B}$ for the shape of the footing

$$\Gamma_{L/B} = f_{L/B}\Gamma_{L/B=1} \tag{7}$$

Eq. (6) indicates that the ratio of $\Gamma_{L/B}/\Gamma_{L/B=1}$ is also the ratio of footing pressures $p_{f(L/B)}/p_{f(L/B=1)}$ since the pressuremeter pressure will be the same. This ratio was calculated for each value of $s/B$ and gave the corresponding value of $f_{L/B}$ (Fig. 12). The values of $f_{L/B}$ show some variation but in the interest of keeping the method simple, it was decided to recommend a single average value of $f_{L/B}$ for each value of $L/B$. This lead to the regression of Fig. 13

$$f_{L/B} = = 0.8 + 0.2B/L \tag{8}$$

Also shown in Fig. 13 for comparison purposes are previous shape factors from various authors and some experimental data. As can be seen the recommendations collected vary significantly. The values found in this study match well with Meyerhof's recommendations and with load tests performed by FHwA.

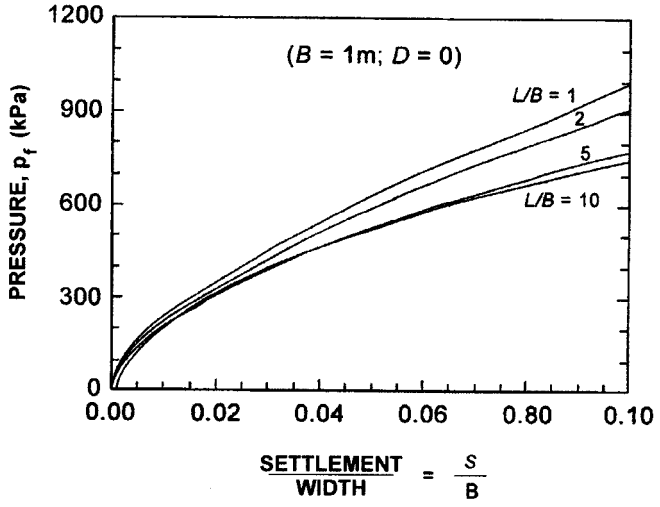


**Fig. 11.** Pressure versus normalized settlement for footings with different shapes

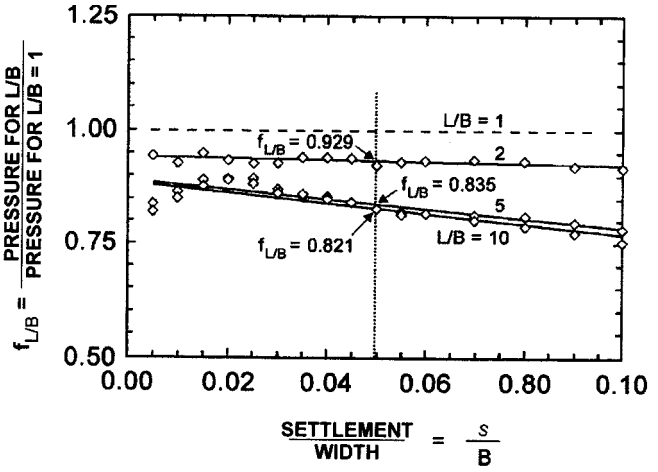


**Fig. 12.** Influence factor for footing shape as a function of normalized settlement

### Eccentricity of the Load

Simulations were performed for $e/B$ ratios (eccentricity to width ratios) equal to 0, 1/16, 2/16, 4/16, and 6/16. Fig. 14 shows an example mesh including the footing and indicates that the footing does not settle evenly with one edge (the critical edge) settling more than the center of the footing. Nevertheless, the footing pressure $p_f$ was always taken as the load divided by the total area of the footing. If the $\Gamma$ function for zero eccentricity is $\Gamma_{e=0}$ and if the $\Gamma$ function for an eccentricity $e$ is $\Gamma_e$, then the influence factor for eccentricity $f_e$ is given by

$$\Gamma_e = f_e\Gamma_{e=0} \tag{9}$$

As in the case of the shape, the $f_e$ values did not vary much with $s/B$ and a single average value was used for each eccentricity case. Fig. 15 shows the values of $f_e$ as a function of $e/B$ from which the following regressions were obtained

$$\text{At the critical edge} \quad f_e = 1 - (e/B)^{0.5} \tag{10}$$

$$\text{At the center} \quad f_e = 1 - 0.33(e/B) \tag{11}$$

Also shown on Fig. 15 for comparison purposes are previous eccentricity factors from various authors and some experimental data. The proposed factor $f_e$ in this study matches well with published data by the LCPC (1991) for the center of footing and by Aiban and Znirdacic (1995) for the edge of the footing. Meyerhof's (1953) recommendations fall between the proposed recommendations for the center and the edge of the footing.

### Inclination of the Load

Simulations were performed for inclination angles equal to 0, 10, 20, and 30° from the vertical. Again in this case, the footing does not settle evenly and one edge (the critical edge) settles more than the center. Nevertheless, the footing pressure was taken as the load divided by the total area of the footing. If the $\Gamma$ function for zero inclination is $\Gamma_{\delta=0}$ and the $\Gamma$ function for an inclination $\delta$ is $\Gamma_\delta$, then the influence factor for inclination is $f_\delta$ given by

$$\Gamma_\delta = f_\delta\Gamma_{\delta=0} \tag{12}$$

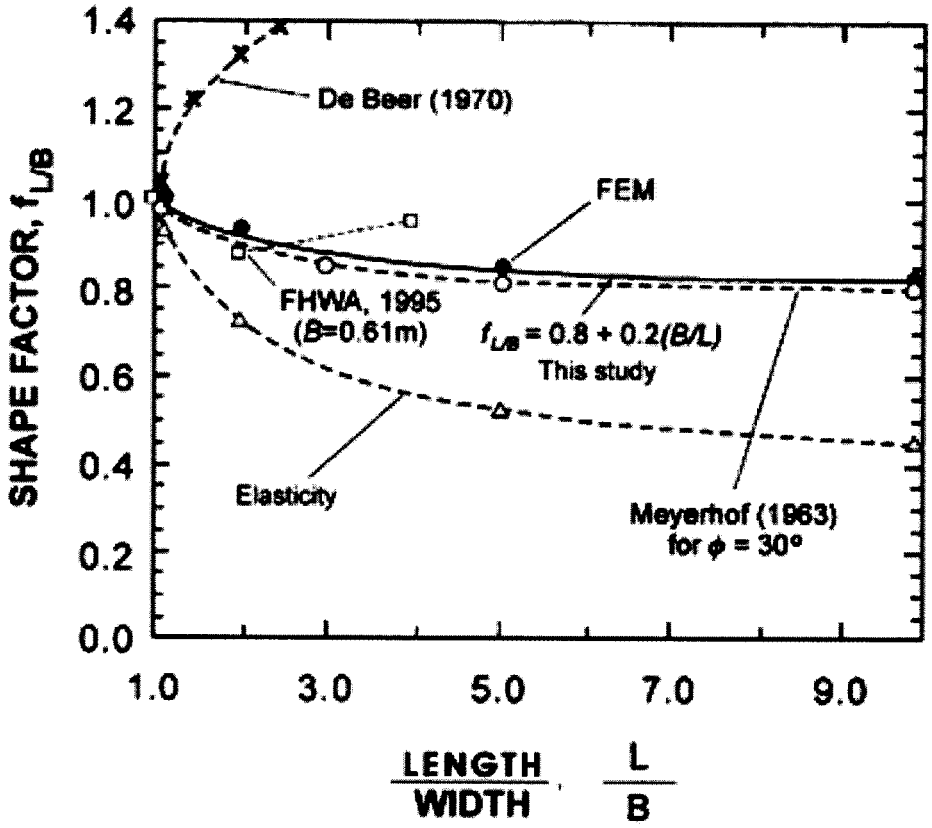


**Fig. 13.** Influence factor for footing shape

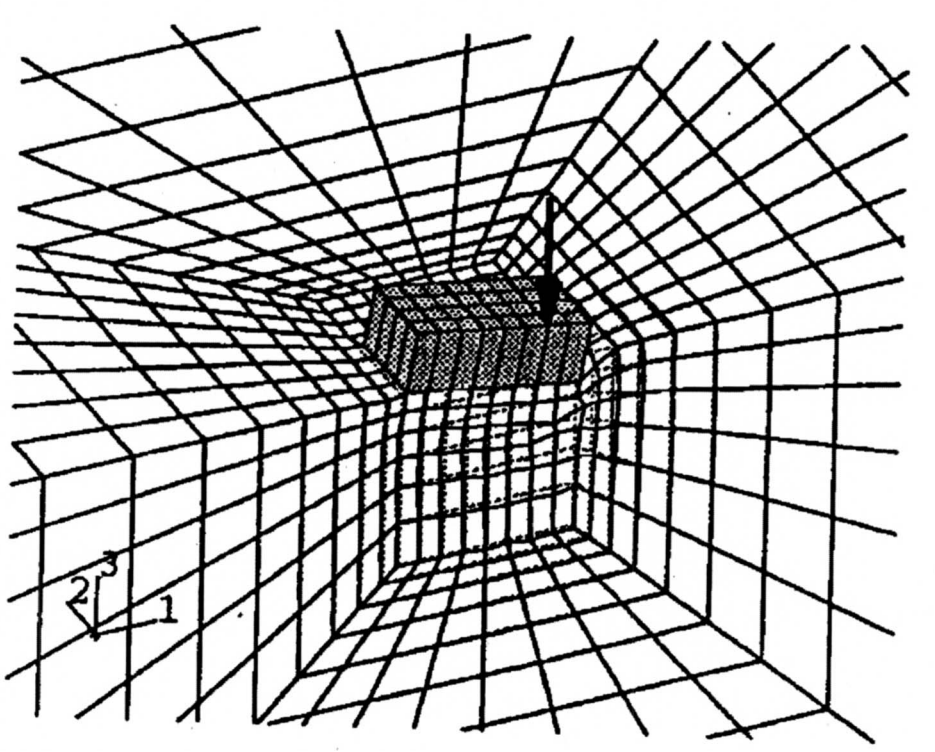


**Fig. 14.** Simulation of a footing subjected to an eccentric load (adapted from Hossain 1996).

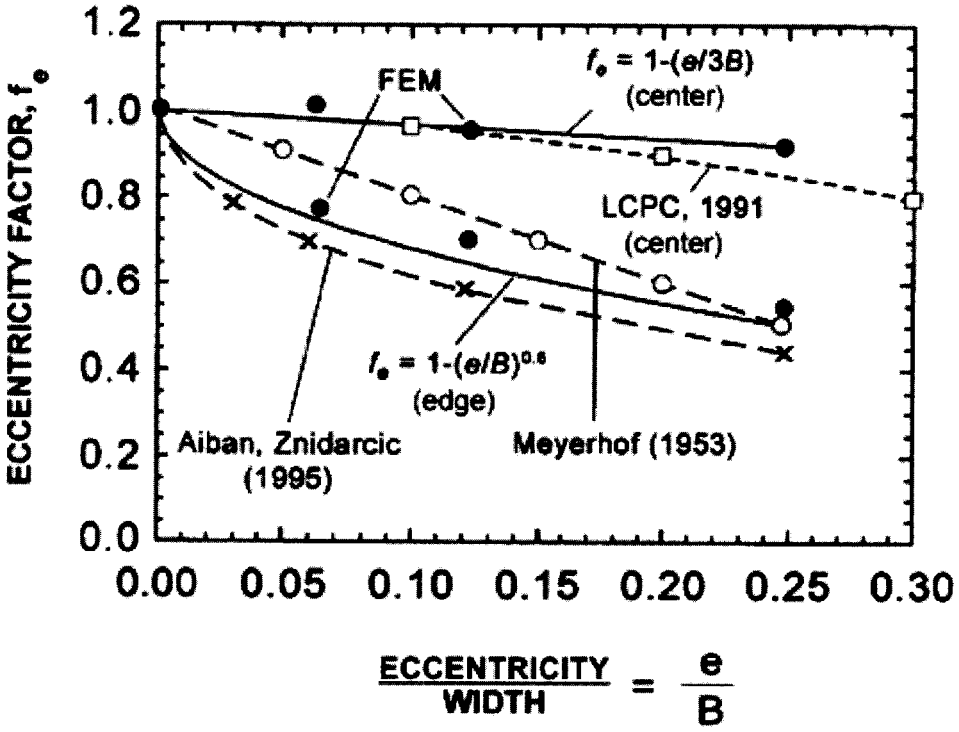


**Fig. 15.** Influence factor for load eccentricity

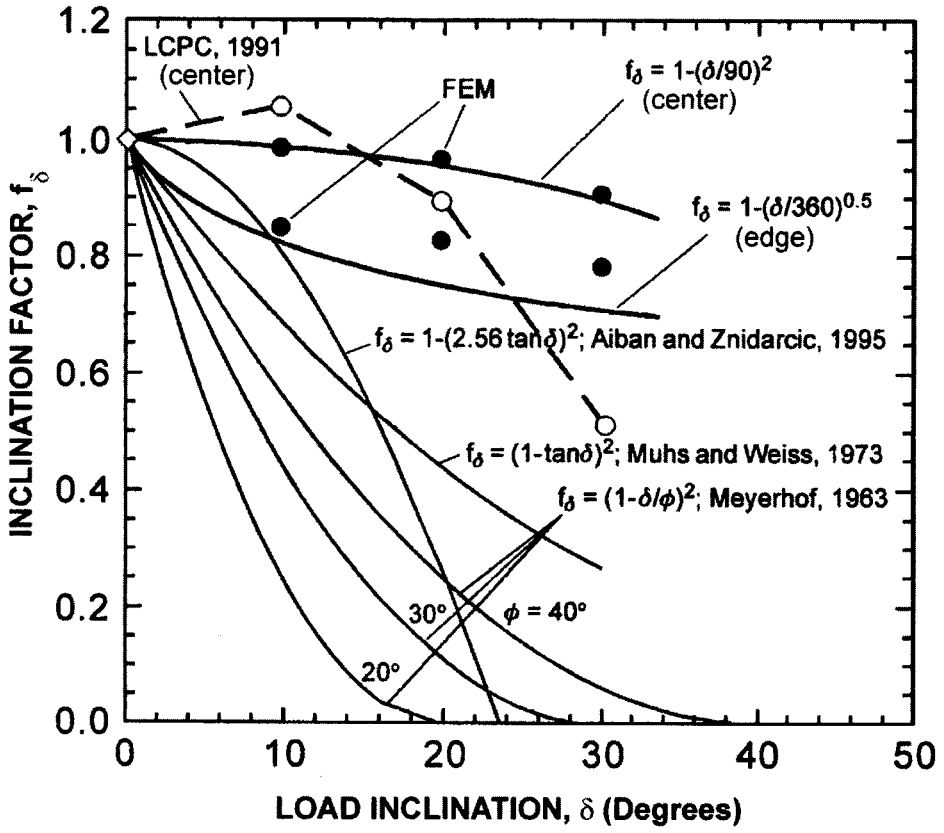


**Fig. 16.** Influence factor for load inclination

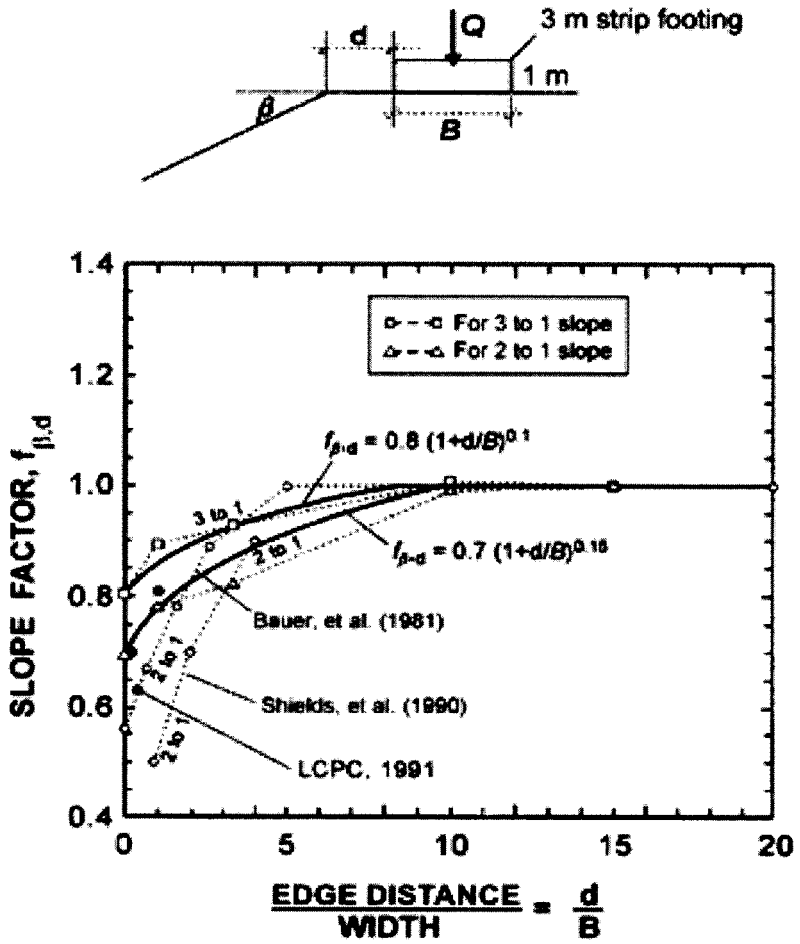


**Fig. 17.** Influence factor for the proximity of a slope

As in the case of the eccentricity, the $f_\delta$ values did not vary much with $s/B$ and a single average value was used for each inclination case. Fig. 16 shows the values of $f_\delta$ as a function of δ from which the following regressions were obtained

$$\text{At the critical edge} \quad f_\delta = 1 - (\delta/360)^{0.5} \tag{13}$$

$$\text{At the center} \quad f_\delta = 1 - (\delta/90)^2 \tag{14}$$

Also shown on Fig. 16 for comparison purposes are previous inclination factors from various authors and some experimental data. The recommendations from this study are close to the measurements made by the LCPC (1991) and indicate that up to an inclination of 20°, there is little reduction in capacity. The results from Meyerhof (1953), Muhs and Weiss (1973), and Aiban and Znidarcic (1995) recommend a much larger reduction.

### *Proximity of a Slope*

Simulations were performed for a 3-m-wide strip footing near a 2 to 1 slope ($\beta = 26.6°$) and a 3 to 1 slope ($\beta = 18.4°$). The foundation was always on the ground surface but the ratio $d/B$ of the distance to the slope and the footing width (Fig. 17) was taken equal to 0, 1, 3.33, 10, and 15. If the Γ function for the absence of slope is $\Gamma_{\beta=0}$ and the one for a slope angle β and a distance $d$ is $\Gamma_{\beta,d}$, then the influence factor is $f_{\beta,d}$ such that

$$\Gamma_{\beta,d} = f_{\beta,d}\Gamma_{\beta=0} \tag{15}$$

Contrary to other cases, the $f_{\beta,d}$ varied significantly with $s/B$ and it was decided to select the most conservative value (larger displacements predicted). Fig. 17 shows those values from which the following equations were derived

$$\text{For a 3 to 1 slope} \quad f_{\beta,d} = 0.8(1 + d/B)^{0.1} \tag{16}$$

$$\text{For a 2 to 1 slope} \quad f_{\beta,d} = 0.7(1 + d/B)^{0.15} \tag{17}$$

Note that for $d/B = 10$ the slope has no influence. Also shown on Fig. 17 for comparison purposes are previous slope factors from various authors and some experimental data. The recommendations in this study match reasonably well the load test results from the LCPC (1991), Bauer et al. (1981), and Shields et al. (1990). Exception is noted for small edge distances ($d/B < 3$) where the Bauer et al. (1981) and Shields et al. (1990) studies give more severe reductions.

### *Superposition*

Now that the individual effects have been estimated through the individual influence factors, it is necessary to combine their effect when more than one influence factor is to be accounted for. No

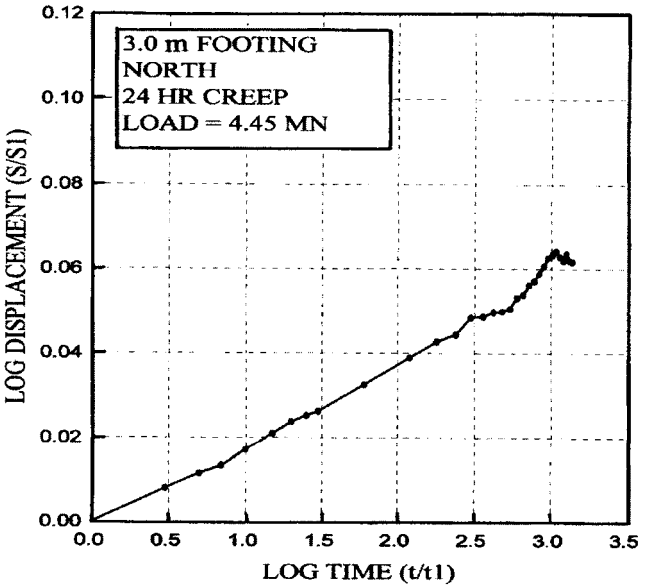


**Fig. 18.** Settlement versus time observed for a $3 \times 3$ m spread footing test (adapted from Briaud and Gibbens 1999)

detailed simulation study was undertaken to investigate the superposition process; this remains to be done. The individual influence factors developed in this study apply to the complete load settlement curve. These influence factors have been compared in the previous sections with similar individual influence factors developed for the ultimate bearing capacity (Meyerhof 1963; Brinch Hansen 1970). The same authors recommend that cases presenting a combination of influences be solved by multiplying the individual influence factors to obtain a combined influence factor (Fang 1991). Six 3D nonlinear FEM simulations were performed involving the combination of several factors including shape, inclination, and eccentricity (Hossain 1996). The load settlement curves generated by this direct simulation of combined cases were compared to the load settlement curves obtained by multiplying the pressure axis of the load settlement curve for the reference case by the combined influence factor. The reference case was the case of a square footing on flat ground subjected to a centered vertical load. The combined influence factor was obtained by multiplying the individual influence factors. In five out of the six cases the results indicated that the multiplication approach is conservative as it yielded larger settlements for the same pressure. In the absence of other evidence, the classical multiplication approach is recommended here

$$p_f = f_{L/B} f_e f_\delta f_{\beta,d} \Gamma p_p \tag{18}$$

## Long-Term Settlement

The load settlement curves predicted by the new approach are calibrated against load tests that typically bring the footing to a large displacement in a matter of hours. Yet the foundations to be designed using that new approach are typically designed for much longer time periods (say 50 years). Since settlement in soils is a time-dependent phenomenon, the effect of time on the settlement of footings in sands was addressed. The chosen model is one that has been used for many years to address the problem of time-dependent effects in soils (Briaud and Garland 1985). This model is

$$s(t)/s(t_1) = (t/t_1)^n \tag{19}$$

where $s(t)$ and $s(t_1)$=settlements after a time equal to $t$ and $t_1$, respectively; and $n$=time dependency exponent. The time $t_1$=reference time corresponding to the PMT test and is set at 1 min.

This model was found to fit well with the observations of settlement versus time made on the large scale footings tested at Texas A&M University (see Fig. 18; Briaud and Gibbens 1999). Indeed, Eq. (19) indicates a linear variation on a log–log scale and Fig. 18 shows that the measurements corroborate such linearity. The time dependency exponent $n$ typically varies from 0.005 to 0.03 for sands and from 0.02 to 0.08 for clays (Briaud 1992). It is recommended that site specific $n$ values be obtained by creep pressuremeter testing (Briaud 1992); if this is not convenient, a value of 0.03 seems conservative for sands in most cases.

## Step-by-Step Procedure and Reliability

The steps for the new load settlement curve method follow:

1. Perform preboring pressuremeter tests within the zone of influence of the footing.
2. Plot the PMT curves as pressure $p_p$ on the cavity wall versus relative increase in cavity radius $\Delta R/R_o$ for each test. Extend the straight line part of the PMT curve to zero pressure and shift the vertical axis to the value of $\Delta R/R_o$ where that straight line intersects the horizontal axis; re-zero that axis (Fig. 8). This is done to correct the origin for the initial expansion of the pressuremeter to fill the borehole.
3. Develop the mean pressuremeter curve of all the PMT curves within the depth of influence of the footing by using an averaging technique based on the influence diagram shown on Fig. 19 (Schmertmann 1970).
4. Transform the PMT curve point by point into the footing curve by using

$$s/B = 0.24 \Delta R/R_o \tag{20}$$

$$p_f = f_{L/B} f_e f_\delta f_{\beta,d} \Gamma p_p \tag{21}$$

$$\text{Shape factor} \quad f_{L/B} = 0.8 + 0.2(B/L) \tag{22}$$

$$\text{Eccentricity factor} \quad f_e = 1 - 0.33(e/B) \quad \text{center} \tag{23}$$

$$f_e = 1 - (e/B)^{0.5} \quad \text{edge} \tag{24}$$

$$\text{Inclination factor} \quad f_\delta = 1 - [\delta(\text{degrees})/90]^2 \quad \text{center} \tag{25}$$

$$f_\delta = 1 - [\delta(\text{degrees})/360]^{0.5} \quad \text{edge} \tag{26}$$

$$\text{Slope factor} \quad f_{\beta,d} = 0.8(1 + d/B)^{0.1} \quad 3 \text{ to } 1 \text{ slope} \tag{27}$$

**Note: the mean PMT curve is obtained point by point by using a weighted average of the pressures for each value of the relative increase in cavity radius. The weighting factors are equal to the areas tributary to each test under the influence diagram. For the example below, the mean PMT pressure $p_m$ is given by the combination of the PMT pressures $p_1$, $p_2$, and $p_3$ of the PMT tests performed at depths $z_1$, $z_2$, and $z_3$ respectively.**

$$p_m = \frac{0.416}{1.125}p_1 + \frac{0.394}{1.125}p_2 + \frac{0.315}{1.125}p_3$$

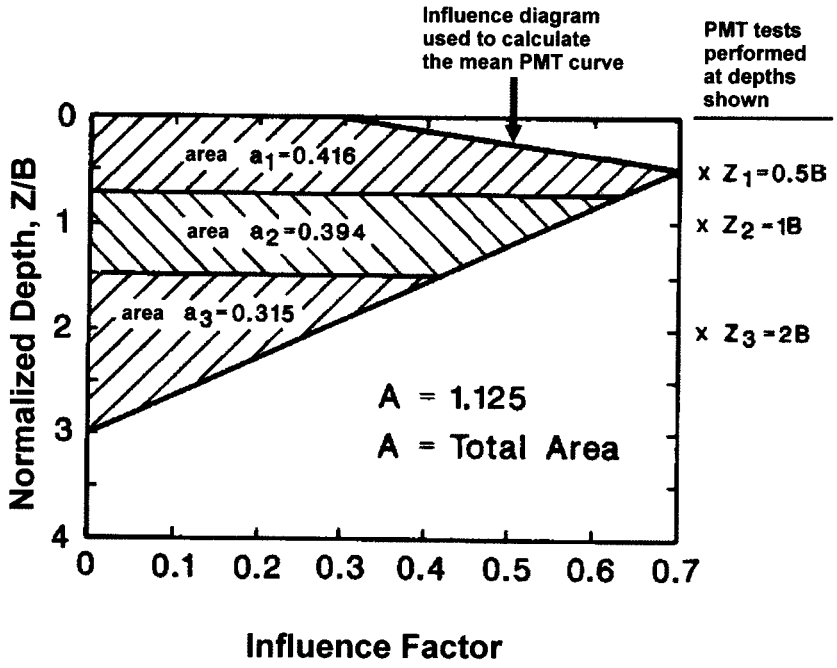


**Fig. 19.** Averaging the pressuremeter curves within the footing zone of influence (adapted from Jeanjean 1995)

$$f_{\beta,d} = 0.7(1 + d/B)^{0.15} \quad \text{2 to 1 slope} \tag{28}$$

5. Generate the short term load settlement curve for the footing from the normalized curve.
6. Generate the long term load settlement curve by multiplying all settlement values by the factor $(t/t_1)^n$ where $t$=design life, $t_1$ is 1 h, and $n$=time exponent obtained from PMT tests or set equal to 0.03 as the default value.

Fig. 20 shows an example of calculations using the new approach. Predictions of the short-term settlement using the new method were compared to measurements of settlement made for the spread footings of the database. Note that it would be much more desirable to use a completely separate database to evaluate the method. Fig. 21 shows that comparison for the 0.01B level of displacement and the 0.1B level of displacement. As can be seen the method is nearly always on the safe side when the design function is used (predicted settlements larger than observed settlements). If this method is to be used as a prediction method the mean $\Gamma$ function should be used, while if the new method is to be used as a design method the design $\Gamma$ function (mean minus one standard deviation) should be used.

## Conclusions

The following conclusions are based and limited to the extent of the data presented. This data includes soil strength profiles that are constant with depth or increase linearly with depth. This method has not been verified for cases where the profile within the footing depth of influence consists of layers with significantly different stiffness and strength properties.

1. For a spread footing in sand, there is no scale nor embedment effect on the normalized load settlement curve; this curve is a plot of the mean pressure under the footing normalized to a parameter representing the soil strength within the zone of influence of the footing versus the settlement divided by the footing width. This curve is a unique property of the soil alone.
2. The general bearing capacity equation for sands corresponds to a soil strength profile which increases linearly with depth; in this case, the bearing capacity factors $N_\gamma$ and $N_q$ are constant and the equation describes properly the influence of $B$ and $D$ on the footing capacity. For any other soil strength profile including the common profile of constant strength

**PROBLEM:** A bridge abutment rests on a shallow foundation 15 m long and 3 m wide. The foundation is subjected to a vertical and centered load equal to 9000 kN. The lateral earth pressure generates a load of 900 kN on the back of the abutment. The resultant of the two forces has an eccentricity equal to 0.2 m. The soil is a sand characterized by an average pressuremeter curve.

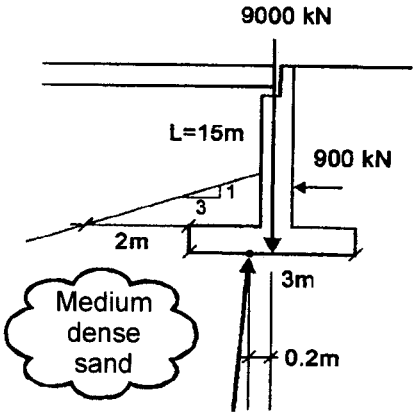


**SOLUTION:** Load-Settlement Curve Method

$$f_{L/B} = 0.8 + 0.2 \times 3/15 = 0.840$$

$$f_e = 1 - 0.33 \times 0.2/3 = 0.978$$

$$f_\delta = 1 - \left(\frac{\text{Arc tan } 900/9000}{90}\right)^2 = 0.996$$

$$f_{\beta,d} = 0.8\,(1 + 2/3)^{0.1} = 0.842$$

$$f = f_{L/B}\, f_e\, f_\delta\, f_{\beta,d} = 0.689$$

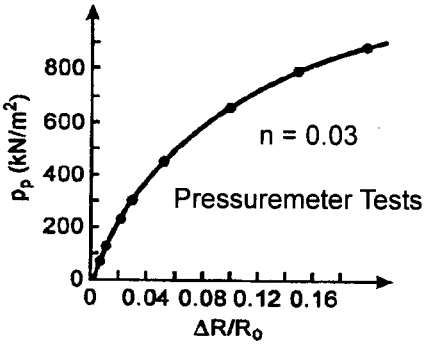


| $\Delta R/R_o$ | $p_p$ (kN/m²) | $s/B$ | $s$ (mm) | $\Gamma$ | f | $p_f$ (kN/m²) | Q (MN) |
|---|---|---|---|---|---|---|---|
| 0.005 | 60 | 0.0012 | 3.6 | 2.25 | 0.689 | 93.0 | 4.18 |
| 0.01 | 120 | 0.0024 | 7.2 | 2.02 | 0.689 | 167.0 | 7.51 |
| 0.02 | 220 | 0.0048 | 14.4 | 1.72 | 0.689 | 260.7 | 11.73 |
| 0.03 | 300 | 0.0071 | 21.3 | 1.54 | 0.689 | 318.3 | 14.32 |
| 0.05 | 450 | 0.0119 | 35.7 | 1.33 | 0.689 | 412.3 | 18.55 |
| 0.10 | 650 | 0.0238 | 71.4 | 1.15 | 0.689 | 515.0 | 23.17 |
| 0.20 | 800 | 0.0357 | 107.1 | 1.02 | 0.689 | 562.2 | 25.30 |
| 0.30 | 900 | 0.0476 | 142.8 | 0.97 | 0.689 | 601.5 | 27.07 |

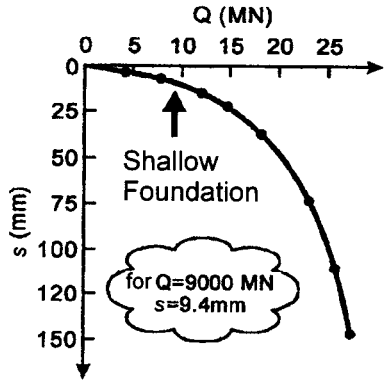


**Settlement at 50 years.**

$$s_{50yrs} = s_{1hr} \times \left(\frac{50 \times 365 \times 24}{1}\right)^{0.03} = 9.4 \times 1.476 = 13.9 \text{ mm}$$

**Fig. 20.** Example calculations

with depth, this equation should not be used because the hypotheses on which the equation is based are not verified and it does not represent the true variation of the ultimate bearing capacity with depth and with embedment.

3. A new method is proposed to alleviate this problem and to obtain the complete load settlement curve for a spread footing on sand from the pressuremeter curve. The problem solved is the one of a rectangular footing located near a slope and subjected to an eccentric and inclined load applied for a given period of time. The development of the method is based on load test data (24 spread footing load tests), numerical simulations (20 FEM runs), and an established time effect model.


## Acknowledgments

Many organizations and individuals have helped over the last ten years in the development of this method. They are all thanked very sincerely for their valuable contributions. The students at Texas A&M University included Robert Gibbens, Philippe Jean-jean, Kabir Hossain, Jayson Barfknecht, Jonghyub Lee, and Remon Abdelmalek. The main sponsor was the Federal Highway Administration with Al DiMillio and Mike Adams. Various colleagues have contributed load test data including Jean-Pierre Magnan and Yves Canepa (France), R. Larsson (Sweden), Nabil Ismael (Kuwait), Kenneth Tand (USA), Alan Lutenegger (USA), Hon-Yim Ko (USA), and Recep Yilmaz (USA).

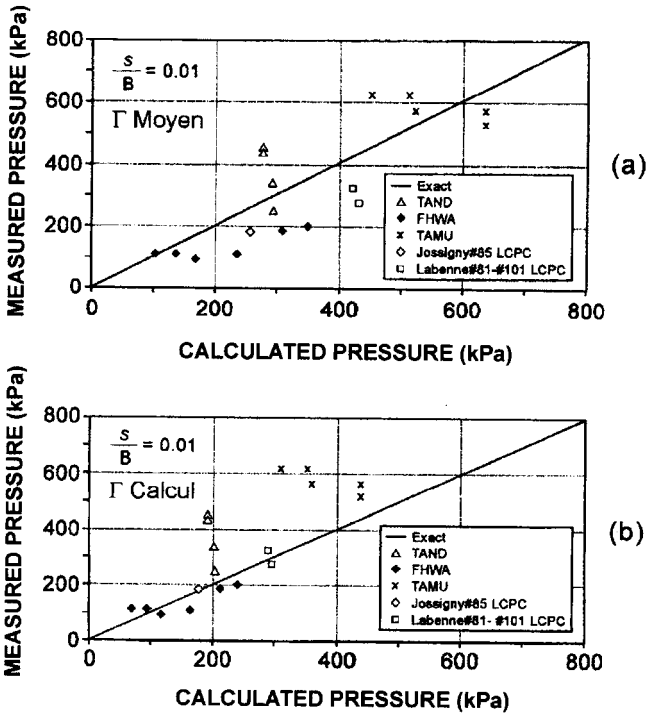


**Fig. 21.** Pressure measured and predicted for a settlement of 0.01B using: (a) the mean Γ function; (b) the design Γ function

## References


ABAQUS. (1991). *Theory manual*, Hibbit, Karlson & Sorensen Inc., R.I.

Aiban, S. A., and Znidarcic, D. (1995). "Centrifugal modeling of bearing capacity of shallow foundations on sands." *J. Geotech. Engrg.*, 121(10), 704–712.

Bauer, G. E., Shields, D. H., Scott, J. D., and Gruspier, J. E. (1981). "Bearing capacity of footings in granular slopes." *Proc., 10th Int. Conf. of Soil Mechanics and Foundation Engineering*, Stockholm, Sweden, Balkema Publishers, Rotterdam, The Netherlands, Vol. 2, 33–36.

Bolton, M. D. (1986). "The strength and dilatancy of sands." *Geotechnique*, 36(1), 65–78.

Bolton, M. D., and Lau, C. K. (1989). "Scale effects in the bearing capacity of granular soils." *Proc., 12th Int. Conf. of Soil Mechanics and Foundation Engineering*, Balkema Publishers, Rotterdam, The Netherlands, Vol. 2, 895–898.

Briaud, J.-L. (1992). *The pressuremeter*, Balkema Publishers, Rotterdam, The Netherlands, 322.

Briaud, J.-L., and Garland, E. (1985). "Loading rate method for pile response in clay." *J. Geotech. Engrg.*, 111(3), 319–335.

Briaud, J.-L., and Gibbens, R. M. (1999). "Behavior of five large spread footings in sand." *J. Geotech. Geoenviron. Eng.*, 125(9), 787–796.

Briaud, J.-L., and Jeanjean, P. (1994). "Load settlement curve method for spread footings on sand." *Geotech. Spec. Publ.*, A. T. Yeung and G. Y. Felio, eds., ASCE, Reston, Va., 1774–1804.

Brinch Hansen, J. (1970). "A revised and extended formula for bearing capacity." *Bulletin No. 11*, Danish Geotechnical Institute, Copenhagen.

Consoli, N. C., Schnaid, F., and Milititsky, J. (1998). "Interpretation of plate load tests on residual soil site." *J. Geotech. Geoenviron. Eng.*, 124(9), 857–867.

Corté, J. F. (1980). "Small scale testing in geotechnical engineering." *Proc., 12th Int. Conf. of Soil Mechanics and Foundation Engineering*, Balkema Publishers, Rotterdam, The Netherlands, Vol. 4, 2553–2571.

De Beer, E. E. (1965). "The scale effect on phenomenon of progressive rupture in cohesionless soils." *Proc., 6th Int. Conf. Soil Mechanics and Foundation Engineering*, Univ. of Toronto, Canada, Balkema Publishers, Rotterdam, The Netherlands, Vol. 2, 13–17.

De Beer, E. E. (1970). "Experimental determination of shape factor and bearing capacity factors of sand." *Geotechnique*, 20(4), 387–411.

Duncan, J. M., and Chang, C.-Y. (1970). "Nonlinear analysis of stresses and strain in soils." *J. Soil Mech. and Found. Div.*, 96(5), 1629–1653.

Fang, H. Y., ed. (1991). *Foundation engineering handbook*, 2nd Ed., Van Nostrand Reinhold, New York, 923.

Garnier, J. (1997). "Validating physical and numerical models: Scale effect problems." *ICSMFE*, 3, 659–663.

Graham, J., and Hovan, J.-M. (1986). "Stress characteristics for bearing capacity in sand using a critical state model." *Can. Geotech. J.*, 23(2), 195–202.

Habib, P. (1985). "Effet de taille et surfaces de glissement." *Revue Française de Géotechn*, 31(2), 5–10.

Hettler, A., and Gudehus, G. (1988). "Influence of the foundation width on the bearing capacity factor." *Soils Found.*, 28(4), 81–92.

Hossain, K. M. (1996). "Load settlement curve method for footings in sand at various depths, under eccentric or inclined loads, and near slopes." Ph.D. thesis, Texas A&M Univ., Dept. of Civil Engineering, College Station, Tex.

Ismael, N. F. (1985). "Allowable pressure from loading tests on kuwaiti soils." *Can. Geotech. J.*, 22(2), 151–157.

Jeanjean, P. (1995). "Load settlement curve method for spread footings on sand from the pressuremeter test." Ph.D. thesis, Texas A&M Univ., Dept. of Civil Engineering, College Station, Tex.

Khebib, Y., Caneépa, Y., and Magnan, M.-P. (1997). "Base de Données de Fondations Superficielles SHALDB: Essais des Laboratoires des Ponts et Chaussées." *Juin 1997*, Laboratoire Central des Ponts et Chaussées, Paris, France.

Kimura, T., Kusakabe, O., and Saitoh, K. (1985). "Geotechnical model tests of bearing capacity problems in a centrifuge." *Geotechnique*, 35(1), 33–45.

Kutter, B. L., Abghari, A., and Cheney, J. A. (1988). "Strength parameters for bearing capacity of sand." *J. Geotech. Engrg.*, 114(4), 491–498.

Larsson, R. (1997). "Investigations and load tests in silty soils." *Rep. No. 54*, Swedish Geotechnical Institute, Roland Offset AB, Linkoping, Sweden.

Mayne, P. W., and Poulos, H. G. (1999). "Approximate displacement influence factors for elastic shallow foundations." *J. Geotech. Geoenviron. Eng.*, 125(6), 453–460.

Meyerhof, G. G. (1953). "The bearing capacity of foundations under eccentric and inclined loads." *Proc., 3rd Int. Conf. of Soil Mechanics and Foundation Engineering*, Balkema Publishers, Rotterdam, The Netherlands, Vol. 1, 440–445.

Meyerhof, G. G. (1963). "Some recent research on the bearing capacity of foundations." *Can. Geotech. J.*, 1(1), 16–26.

Muhs, H. (1965). "On the phenomenon of progressive rupture in connection with the failure load: Discussion." *Proc., 6th Int. Conf. of Soil Mechanics and Foundations Engineering*, Vol. 3, 419–421.

Muhs, H., and Weiss, K. (1973). "Inclined load tests on shallow strip footings." *Proc., 8th Int. Conf. of Soil Mechanics and Foundation Engineering*, Vol. 1, 173–179.

Ovesen, N. K. (1975). "Centrifugal testing applied to bearing capacity problems of footings on sand." *Geotechnique*, 25(2), 354–401.

Perkins, S. W., and Madson, C. R. (2000). "Bearing capacity of shallow foundations on sand: A relative density approach." *J. Geotech. Geoenviron. Eng.*, 126(6), 521–530.

Pu, J.-L., and Ko, H.-Y. (1988). "Experimental determination of bearing capacity in sand by centrifuge footing tests." *Proc., Centrifuge '88*, J.-P. Corte, ed., Balkema, Rotterdam, The Netherlands, 293–299.

Seed, R. B., and Duncan, J. M. (1983). "Soil-structure interaction effects of compaction-induced stresses and deflections." *Rep. No. UCB/GT/83-06*, Univ. of California, Berkeley.

Shields, D., Chandler, N., and Garnier, J. (1990). "Bearing capacity of foundations in slopes." *J. Geotech. Engrg.*, 116(3), 528–537.
Shiraisi, S. (1990). "Variation in bearing capacity factors of dense sand assessed by model loading tests." *Soils Found.*, 1(30), 17–26.
Steenfelt, J. S. (1977). "Scale effect on bearing capacity factor $N_\gamma$." *Proc., 9th Int. Conf. of Soil Mechanics and Foundations Engineering*, Balkema Publishers, Rotterdam, The Netherlands, Vol. 1, 749–752.
Tand, K. E., Funegard, E., and Warden, P. (1994). "Footing load tests on sand." *Proc., Settlement '94 Specialty Conf.*, ASCE Geotechnical Specialty Publication No. 40, Vol. 1, 164–178, Reston, Va.
Terzaghi, K. (1943). *Theoretical soil mechanics*, Wiley, New York, 510.
Terzaghi, K., Peck, R. B., and Mesri, G. (1996). "Soil mechanics in engineering practice." 3rd Ed., Wiley, New York, 549.
Yamaguchi, H., Kimura, T., and Fuji, N. (1976). "On the influence of progressive failure on the bearing capacity of shallow foundations in dense sand." *Soils Found.*, 16(4), 11–22.